

Aircraft Design 1 – Fall 2021

Assignment 3 Wing Design

Student Names and USCIDs:

Instance 1

Hours spent on assignment: 50h



Figure 1.1: Aircraft Render

Aircraft type: Business Jet
Aircraft number: 105

Table 1: Requirements Table

Requirement type	Value	Unit
Payload	900	kg
Range	3200	km
Cruise speed	770	Km/h
Take-off distance	900	m
Landing distance	800	m



Figure 1.2: Aircraft Configuration



Table of Contents

Table of Contents	3
1. Introduction	4
2. Clean Wing Design	4
2.1 Infinite Wing	4
2.2 Finite Wing and Mean Aerodynamic Chord	5
2.3 Airfoil Selection	6
2.4 Validity and sanity checks	8
2.4.1 Pitchup Tendency	8
2.4.2 Sweep Angle	9
2.4.3 Aspect Ratio	9
2.4.4 Taper Ratio	10
2.4.5 Mach Drag Divergence	10
2.4.6 Miscellaneous Parameters	11
2.5 Clean Wing Lift Curve	11
3. High Lift Devices	14
3.1 Take-off and Landing conditions	14
3.2 High lift device approach selection	15
3.3 Device Sizing	15
3.4 CL-a Curve for Flapped Wing	17
4.1 Wing Fuel Tank	19
4.2 Total Fuel Storage Capacity	20
References	21
Appendix A: Updated Drawings	22
Appendix C: Table of Reference Aircraft	30
Appendix D: Current Aircraft parameters Table	32

1. Introduction

In the following report the aircraft wing configuration and specification are considered, a wing is engineered to fit the criteria introduced in the beginning of the course. The first section focuses on the introductory wing size and geometrical dimensions for a simple wing. The following chapter introduces the high lift devices and ensures the wing satisfies the take-off/landing conditions needed to satisfy the requirements. Chapter 4 will finally focus on the fuel storage for the aircraft within the wings to obtain a volume to satisfy estimated fuel from Assignment 2. This report will also include the updated drawings of the aircraft with the newly designed wing.

2. Clean Wing Design

The initial calculations required to design a wing focus on the basic aerodynamic properties of a simple wing geometry without high lift devices such as flaps or other considerations. An airfoil was chosen and tested using XFOIL to satisfy the flight requirements, from the airfoil a finite wing was then generated and is discussed in this section in detail.

2.1 Infinite Wing

To start the wing calculation the total lift must be determined. The lift is found by multiplying the weight at takeoff by 1.1. This allows compensation for gust and trim effects. The formula for the required lift is shown below in Equation 2.1.

$$L_{MTOW} = 1.1 * W_{MTOW} = 1.1 * 102785 \text{ N} = 113063.5 \text{ N} \quad \text{Eq. 2.1}$$

For the aircraft to fly at the maximum takeoff conditions determined in the previous assignment, the lift needed to be generated by the wing is equal to 113063.5 N. From assignment 2 the wing loading of 2200N/m² is known for the cruise condition of the aircraft. The next step is to determine the wing area from these values of W/S as well as the takeoff weight giving an area of 46.23 m. The formula for lift coefficient can be found utilizing Equation 2.2.

$$C_{L,design} = \frac{2}{\rho_{cruise} * V_{cruise}^2} * \frac{W}{S} \quad \text{Eq. 2.2}$$

The density and velocity are obtained for the cruise conditions of the aircraft and the W/S is found for the average of the cruise by obtaining start and end of cruise W/S values where the surface area of the wing does not change. Finally, the CL design is multiplied by 1.1 to account for gusts and trim loads. By modifying Equation 2.2, Equation 2.3 below can be found.

$$C_{L,design} = 1.1 * \frac{2}{\rho * V_{cruise}^2} * \left(\frac{1}{2} \left[\frac{W}{S_{Start \text{ of } Cruise}} + \frac{W}{S_{End \text{ of } Cruise}} \right] \right) \quad \text{Eq. 2.3}$$

With the above values, the lift coefficient was found to be 0.297. This value however is for that of an unswept wing. Due to the higher cruise speeds at which this aircraft will be traveling, the use of sweep on reference aircraft, and the hindsight of the iterative processes, a leading-edge sweep angle of 20 degrees was chosen. Due to this sweep, the wing will experience a lower effecting free stream velocity of 201 m/s traveling across the wing. A design lift coefficient for an airfoil can be roughly calculated based on the give wing design lift coefficient and chosen sweep angle. This value is given by Equation 2.4 and give a design Cl for the airfoil of 0.337.

$$C_{l,des} = \frac{C_{L,des}}{\cos^2(\lambda)} \quad Eq. 2.4$$

All the current important aircraft and atmospheric parameters relating to the wing design are represented below in Table 2.1.

Table 2.1

PARAMETER	VALUE	UNIT
$W_{start\ cruise}$	98674	N
$W_{end\ cruise}$	74795	N
SWEEP ANGLE LAEADING EDGE	20	degrees
S	46.23	m^2
$\rho\ SEALEVEL$	1.225	kg/m^3
$\rho\ CRUISE$	0.303	kg/m^3
V CRUISE	214	m/s
V EFFECTIVE	201.1	m/s
$C_L\ DES$	0.297	dimensionless
$C_l\ DES$	0.337	dimensionless

2.2 Finite Wing and Mean Aerodynamic Chord

Next, many of the finite characteristics were estimated and later iteratively refined upon. The wing surface area is known to be $46.23\ m^2$ and a high aspect ratio of 10 is desired to obtain efficient aerodynamic characteristics. Given this, a span value, b, may be calculated as given by Equation 2.5 below.

$$b = \sqrt{A * S} = \sqrt{46.23 * 10} = 21.5\ m \quad Eq. 2.5$$

With the total wingspan calculated it can easily be seen that one wing will have a length of 10.75m. The root chord was then chosen to be 3.4 m to obtain a reasonable taper value while maintaining feasible tip chord. The taper value is given by Equation 2.6 while the tip chord can then be found by Equation 2.7.

$$\lambda = \frac{2b}{c_r * A} - 1 = 0.265 \quad Eq. 2.6$$

$$c_t = c_r * \lambda = 0.9\ m \quad Eq. 2.7$$

Now the Mean Aerodynamic Chord (MAC) can be found. First, the spanwise location, Y, is found utilizing geometric relationships given by Equation 2.8, resulting in the location of the MAC from the center of the aircraft.

$$Y = \frac{b}{6} * \frac{1 + 2\lambda}{1 + \lambda} = 4.334\ m \quad Eq. 2.8$$

From there, the MAC length can then be calculated similarly based upon geometric relationships given by Equation 2.9.

$$MAC = \frac{2 * C_r}{3} * \frac{(1 + \lambda + \lambda^2)}{(1 + \lambda)} = 2.392\ m \quad Eq. 2.9$$

The estimated aerodynamic center of a wing for subsonic aircraft called the center of pressure is typically based off of 25% of the MAC. With the calculated MAC value, the center of pressure is

found to be 0.598 m from the leading edge. This value is where the pressure forces such as lift act on the wing.

2.3 Airfoil Selection

The airfoil for the wing was now selected and analysed utilizing the XFOIL software. The online airfoil database Airfoil Tools [1] was utilized to reference airfoils of different types and obtain a point cloud for later reconstruction. For this business jet, a supercritical airfoil was chosen to delay the transonic effects at the desired cruise speed while maintaining a thicker airfoil. The NASA SC(2)-0412 was ultimately chosen. The naming convention for the NASA super critical airfoils led to the selection of this specific airfoil as the first 2 numbers indicate the designed lift coefficient while the last 2 numbers represent the airfoil thickness as a ratio of the chord. To analyse the airfoil, the Reynolds number was calculated for both cruise condition as well as low level/speed (landing) operations utilizing the MAC as the critical distance. The formulas and values for the Reynolds number calculations are given by Equations 2.10 a and b for the cruise and low-level operations respectively.

$$Re = \frac{\rho_{cruise} * V_{cruise} * C_{MAC}}{\mu_{cruise}} = \frac{0.303 * 214 * 2.3923}{1.44216 * 10^{-5}} = 10.8 * 10^6 \quad Eq. 2.10 \text{ a}$$

$$Re = \frac{\rho_{low_speed} * V_{low_speed} * C_{MAC}}{\mu_{low_speed}} = \frac{1.225 * 36.8 * 2.3923}{1.789 * 10^{-5}} = 6.03 * 10^6 \quad Eq. 2.10 \text{ b}$$

XFOIL was then used to analyse the airfoil for the various operating conditions. The airfoil point cloud was loaded into XFOIL where it was broken up into panels to identify the circulation impacting each section. Viscous analysis was enabled, and the corresponding Reynolds numbers were input. The Mach value was left at zero as XFOIL has issues analysing airfoils at higher Mach numbers and compressibility will furthermore be corrected for later. The airfoil was then simulated through various angles of attack (alpha) ranging from -10 to 23 degrees. For each of the two conditions the coefficient of pressure vs chord plot generated by XFOIL, the coefficient of lift vs alpha plot, the moment coefficient vs alpha plot, and the drag polar are displayed below for the cruise condition, on the left, and low-level condition, on the right, in Figures 2.1-2.4 and 2.5-2.8 respectively. Important values are then summarised in Table 2.2 below the figures.

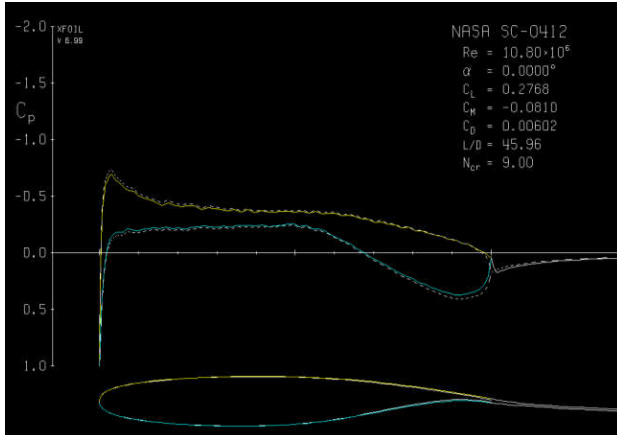


Figure 2.1: Cp Plot at Cruise Conditions

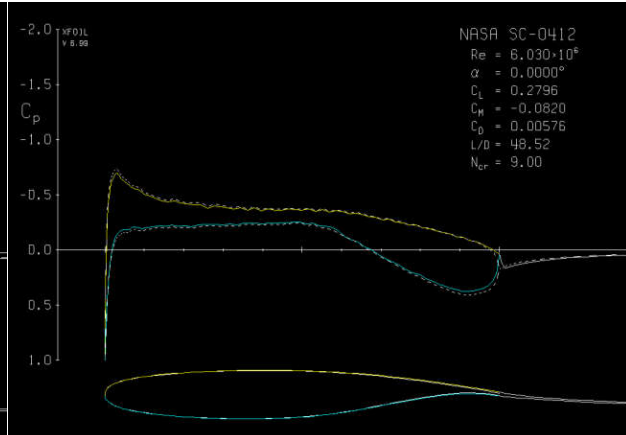


Figure 2.5: Cp Plot for Landing Conditions

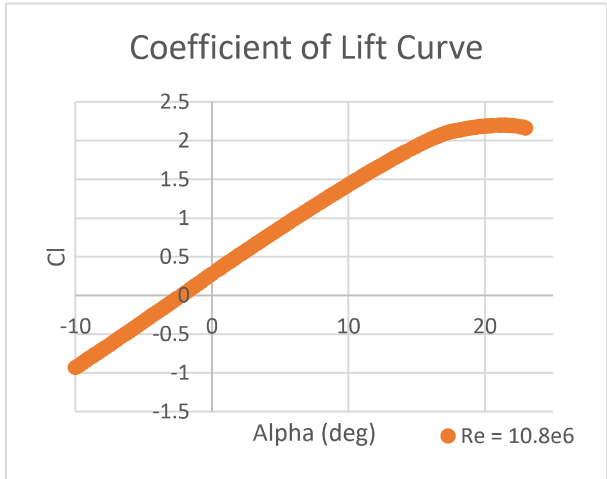
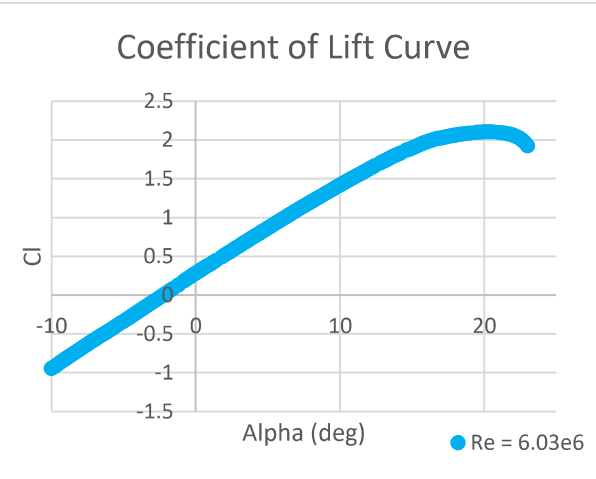
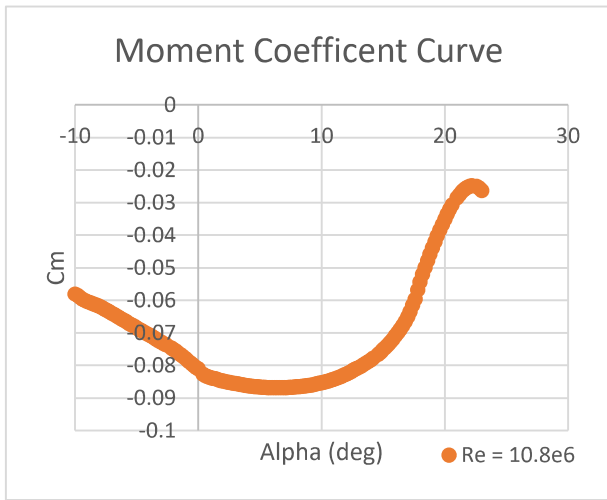
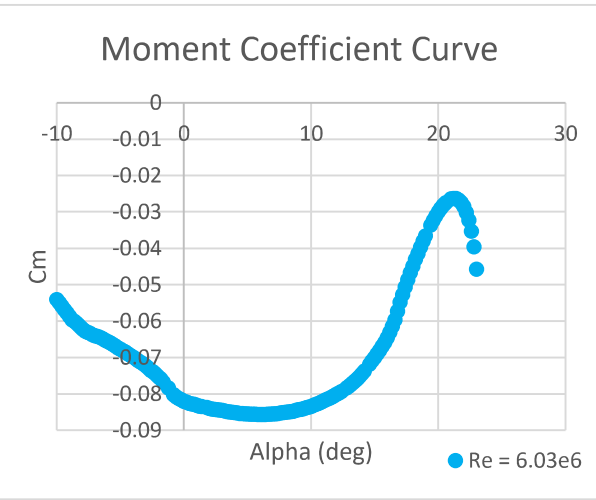
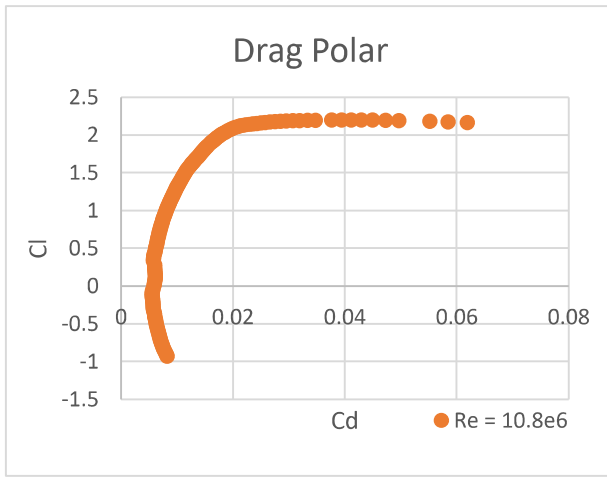
Figure 2.2: C_L Curve at Cruise ConditionFigure 2.6: C_L Curve for Landing ConditionFigure 2.3: C_m Curve at Cruise ConditionFigure 2.7: C_m Curve for Landing Condition

Figure 2.4: Drag Polar at Cruise Condition

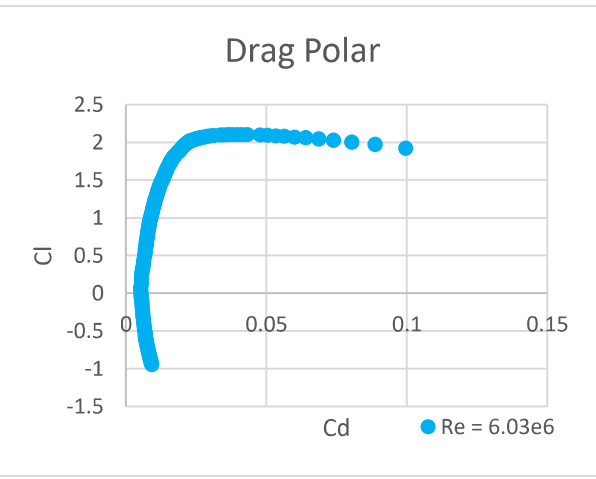


Figure 2.8: Drag Polar for Landing Condition

Table 2.2: NASA SC(2)-0412 Airfoil Parameters

Parameter	Re = 10.8e6	Re = 6.03e6	unit
Min Cp	-0.69	-0.69	
Zero Cl alpha	-2.3	-2.3	degree
Zero alpha Cl	0.2768	0.2796	
Max Cl	2.198	2.103	
Stall Angle	21	20.2	degrees
Min Cd	0.00579	0.55	
Cl at Min Cd	0.353	0.1852	
Alpha at Min Cd	0.6	-0.8	degrees

2.4 Validity and sanity checks

In the following section, the chosen and calculated design characteristics will be checked against that of historical data and other limiting factors to conclude that the chosen wing is acceptable.

2.4.1 Pitchup Tendency

The pitchup tendency of an aircraft is the tendency for an aircraft's nose to continue to raise higher even past the case of a stall. This of course can be detrimental to the flight of an aircraft should an aircraft no be able to bring the nose down for stable flight. Raymer [2] in his book presents a figure utilizing historical data that qualifies the risk of pitchup tendencies based on the aspect ratio, quarter chord sweep angle and flight regime. The sweep angle of a given chord percentage can be found by Equation 2.11.

$$\frac{\Lambda_x}{c} = \arctan \left[\tan(\Lambda_{LE}) - \frac{x}{c} * \frac{2c_r}{b} * (1 - \lambda) \right] \quad Eq. 2.11$$

The quarter chord sweep, $x/c = 0.25$, can then be found to be 17 degrees. These values can be input into Figure 2.9 to find the pitchup tendencies of the aircraft.

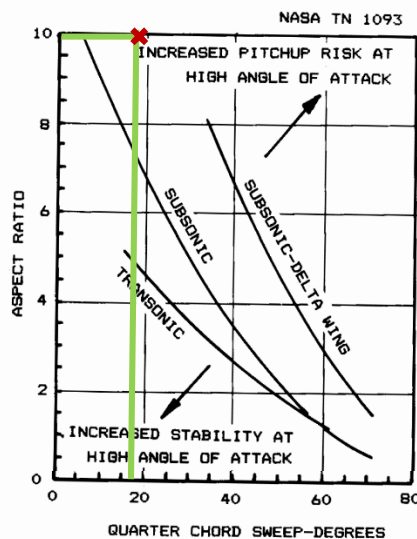


Figure 2.9: Pitchup Risk Chart [2]

From the figure, knowing that this aircraft will be travelling at transonic speeds, it can be seen that there will be an increased risk of pitchup tendencies. It should be noted however that this figure is based solely on contributions from the wing. In reality, a horizontal stabilizer will be utilized to counteract these pitchup tendencies and stabilize the aircraft as a whole.

2.4.2 Sweep Angle

Next, Raymer proposes a historical reference check for the leading-edge sweep angle of the wing vs the expected maximum Mach number. Figure 2.10 can be used to see how the proposed aircraft compares to that of successful aircraft of the past and present.

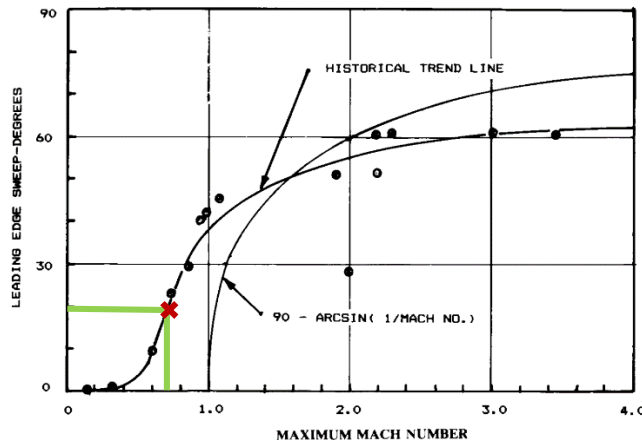


Figure 2.10: Historical Trend for Leading Edge Sweep vs Mach [2]

From the above figure it can clearly be seen that the chosen leading-edge sweep of 20 degrees is right in line with that of historical trends and should not pose any great design challenges.

2.4.3 Aspect Ratio

While a large aspect ratio is highly beneficial for obtaining greater aerodynamic efficiency, larger ratios also pose a much greater structural design challenge. To provide a quick check for feasibility of construction, the cantilever ratio is proposed in Equation 2.12 where t_r is the maximum root thickness found to be 0.408 m and the sweep is of the half chord found using Eq. 2.11 to be 13.9 degrees.

$$\text{Cantilever Ratio} = \frac{b/2}{t_r \cos(\Lambda_{0.5c})} = 27 \quad \text{Eq. 2.12}$$

The calculated cantilever ratio is slightly higher than the typical value of 18 – 22. As cantilever ratios greater than that of 25 typically correspond to braced wing structures, the proposed aircraft will take advantage of such structures. It should be noted for the purposes of this assignment, the lifting characteristics of the brace structure will be ignored, though in reality more care should be devoted to understanding the combined effects of the main wing and brace structure.

2.4.4 Taper Ratio

Aircraft often have taper ratios to take advantage of superior lift distributions across the wing. The closer to an elliptical shape a wing can be the more efficient it is. Raymer for this instance, proposes a figure with historical reference points to check that the taper ratio is close to providing efficient performance. Below is Figure 2.11 which can be used to check the proposed

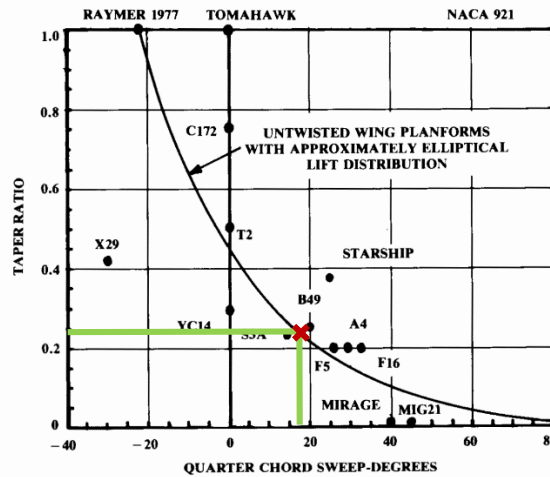


Figure 2.11: Optimal Taper Ratio at Various Quarter Chord Sweep [2]

taper ratio with that of the optimal.

According to the figure, a taper ratio of approximately 0.25 is optimal for achieving a near elliptical lift distribution across the wing. This is extremely close to the found value of 0.265 and should work fine.

2.4.5 Mach Drag Divergence

At transonic speeds there becomes a point where a section of the airfoil can experience supersonic flow before the aircraft breaks the sound barrier. This can cause a drastic increase in drag, so it is important that this occurs beyond the required cruise speed. Various entities have different ways of classifying at what point the drag divergence point is. For this report, Raymer's suggestion of utilizing Boeing's definition as a cruise speed reference point and McDonald Douglas's as a max level speed. Boeing defines the M_{dd} as approximately 0.08 Mach above the critical Mach number, M_{cr} , while Douglas's definition tends to be 0.06 Mach above that of Boeing's according to Raymer [1]. First, a M_{cr} value must be found. The free stream Mach can be related to the C_p in two separate ways. The initial way depends on the isentropic properties of airflow and is given by Equation 2.13.

$$C_{p,cr} = \frac{2}{\gamma M_{cr}^2} \left[\left(\frac{1 + [\frac{\gamma - 1}{2}] M_{cr}^2}{1 + [\gamma - 1)/2]} \right)^{\frac{\gamma}{\gamma - 1}} - 1 \right] \quad Eq. 2.13$$

The second equation is specific to various airfoils and corresponds to the minimum C_p achieved, which is typically more negative for thicker airfoils. This relationship is given by Equation 2.14 below.

$$C_p = \frac{C_{p,0}}{\sqrt{1 - M^2}} \quad Eq. 2.14$$

By plotting these two relationships together from Mach 0 – 1, the point of intersection can be found. This point is the M_{cr} at which a point on the airfoil will experience sonic flow. The M_{cr} based on the two relationships is found to be roughly Mach 0.67. Utilizing Boeing's definition of M_{dd} give as Value of $M_{dd} = 0.75$. This value is well above the required cruise speed of $M = 0.719$, calculated based upon the speed of air at the chosen cruise altitude. Therefore, there should not be large amounts of increased drag due to Mach effects at the required cruise speed. Furthermore, the Douglas definition of M_{dd} which equals 0.81 can be taken to give the max dive speed that the aircraft will be designed for.

2.4.6 Miscellaneous Parameters

There are quite a few more wing parameters that effect performance. While important, the following characteristics have a rather low impact when compared to that of the previously explored parameters but are still worth mentioning.

Wing twist angle describes the twist in the airfoil cross section throughout the span from the root to the tip. Negative angles, known as a washout, where the tip points down more than the root can lead to the tip of the wing stalling after the root of the wing. This is desirable as it allows for use of the ailerons, which are typically located towards the tip, for roll control before the aircraft has completely stalled. For simplicity's sake, a wing twist angle of 0 degrees has been chosen, as it greatly increases the complexity in finding lift curve of the entire wing.

The Dihedral angle is the angle at which the wing point from the horizontal plane. Dihedral, or upwards tilt, can increase an aircraft's stability as during a roll manoeuvre, the lower wing increases its effective span leading to increased lift that opposes the rolling motion. Anhedral is a downward tilt and has the opposite effect of increasing manoeuvrability at the cost of stability. Raymer, in his book, proposes various ranges of Dihedral for differently configured aircraft. For high wing aircraft, it is suggested that an Anhedral value of -2 to -5 degrees is used for swept wing subsonic aircraft. With that in mind, an Anhedral of -4 degrees was chosen for this aircraft.

2.5 Clean Wing Lift Curve

Now that all the wing parameters have been determined, the wing lift curve slope can be created. To obtain the lift curve the curve slope, trim and stall angles need to be found before graphing the lift curve of the wing.

Earlier the wing was analysed at $M = 0$, so before moving forward, the Prandtl Glauert Mach correction must be applied to obtain relevant values. The values for the cruise Mach of 0.719 and landing Mach of 0.108 are presented in Equation 2.15 a and b respectively.

$$\beta_{cruise} = \sqrt{1 - M_{eff}^2} = \sqrt{1 - 0.679^2} = 0.772 \quad Eq. 2.15 \text{ a}$$

$$\beta_{landing} = \sqrt{1 - M_{eff}^2} = \sqrt{1 - 0.102^2} = 0.995 \quad Eq. 2.15\ b$$

Next, the lift curve slope $dCL/d\alpha$ can be found through Equation 2.16. The aspect ratio remains 10 and the efficiency factor is chosen to be 0.95 while the half chord sweep angle of 13.9 degrees or 0.243 radians

$$\frac{dC_L}{d\alpha} = \frac{2 * \pi * A}{2 + \sqrt{4 + \left(\frac{A\beta}{\eta}\right)^2 * \left(1 + \frac{\tan^2 \lambda}{\beta^2}\right)}} \quad Eq. 2.16$$

The lift curve slope for cruise is found to be $dCL/d\alpha = 5.83/\text{rad}$, or $0.102/\text{deg}$. Similarly, the lift curve slope for the landing condition is equal to $dCL/d\alpha = 4.84/\text{rad}$ or $0.0845/\text{deg}$.

Now the trim angle, given by Equation 2.17, for what the wing will need to be set for stable cruise can be found.

$$\alpha_{trim} = \frac{C_{L,des}}{C_{L\alpha}} + \alpha_{0L} \quad Eq. 2.17$$

The value for α_{0L} is obtained as -2.3 degrees, the design lift coefficient is determined as 0.297 from the previous calculations. The C_l alpha is the lift curve slope from the above equation. Thus, the trim angle is calculated to be 0.62 degrees. This trim angle seems to be within range of typical values.

Lastly, the stall angle and CL value can be determined. To find the stall angle the aspect ratio check needs to be considered, as high aspect ratio wings stall differently than smaller ones. A wing is considered to have a high aspect ratio if Equation 2.18 holds true.

$$A > \frac{4}{(C_1 + 1) * \cos \lambda} \quad Eq. 2.18$$

C_1 can be found utilizing Figure 2.12 proposed by Raymer that uses historical data of aircraft [2]. With a taper ratio of 0.26 it can be seen that the C_1 value is very nearly 0.5.

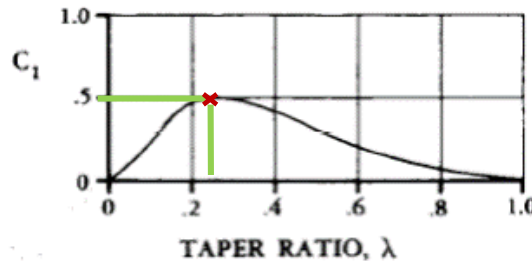


Figure 2.12: Historical Trend for Constant in High Aspect Ratio Definition [2]

The minimum aspect ratio thus becomes 2.84. The chosen aspect ratio of 10 is much greater and therefore can conclusively be considered a high aspect ratio wing. Knowing this, Raymer proposes two historically based trends in Figure 2.13 and 2.14 to find the C_{Lmax}/C_l and delta alpha of C_{Lmax} respectively. To utilize these figures, a delta y value must be found. This value corresponds to the leading-edge sharpness of the airfoil and can be found by taking the

difference in the height of the airfoil between 0.0015c and 0.06c. Utilizing CAD of the airfoil, this value was found to be 3.

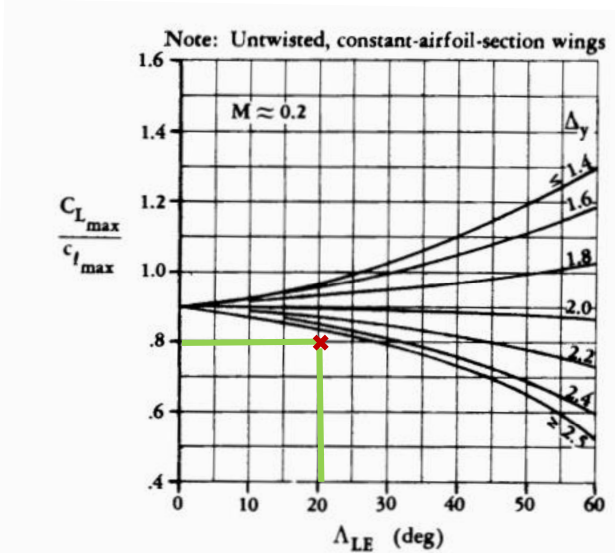


Figure 2.13: Historical Trends for $C_{L\max}/C_{l\max}$ Based on Leading Edge Sharpness [2]

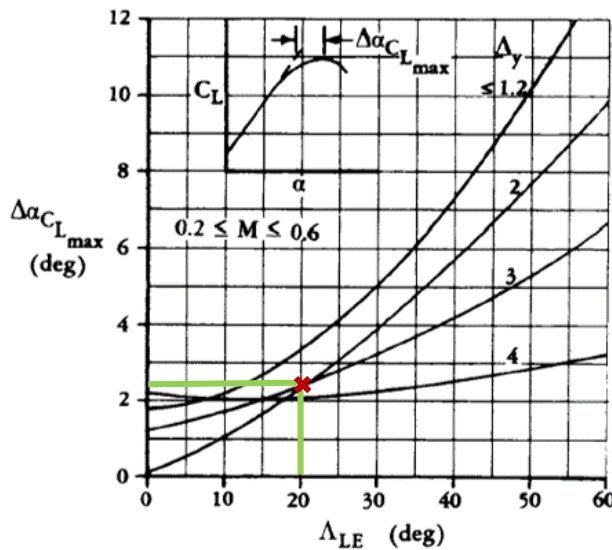


Figure 2.14: Historical Trend for Delta $C_{L\max}$ Based on Leading Edge Sharpness [2]

From these figures the $C_{L\max}/C_{l\max}$ value was found to be 0.8 with a delta $C_{L\max}$ of roughly 2.4 degrees. From here the $C_{L\max}$ value can be determined using Equation 2.19 where the delta $C_{L\max}$ will be ignored due to the low-speed nature of landings.

$$C_{L,max} = \left[\frac{C_{L,max}}{C_{l,max}} \right] * C_{l,max} + \Delta C_{Lmax} = 1.682 \quad Eq. 2.19$$

Finally, the stall angle can be computed with the values previously obtained till this point. The equation for the stall angle is given by Equation 2.20 below.

$$\alpha_s = \frac{C_{L,max}}{C_{La}} + \alpha_{0L} + \Delta\alpha_{CLmax} = 20.02 \quad Eq. 2.20$$

With all the gathered values, the complete CL- α curve for low speeds can be graphed while the linear portion of the cruise condition can be displayed. This curve is displayed in Figure 2.15 with the solid black curve being the complete low speed curve and the dashed line the cruise condition curve slope. Important wing parameters are displayed below in Table 2.3.

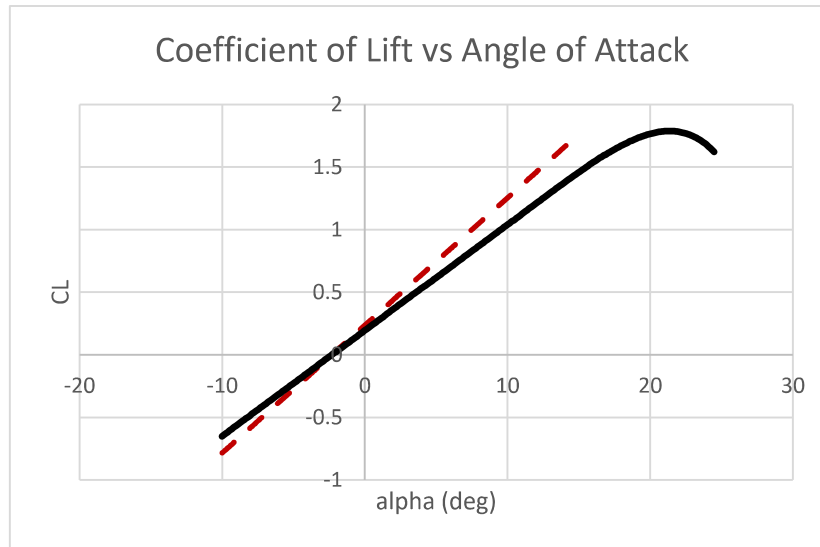


Figure 2.15: Lift Curve Slope for the Proposed Wing

Table 2.3: Wing Parameters

Parameter	Value	Unit
C_{La} Cruise	0.102	CL/degree
C_{La} Landing	0.0845	CL/degree
α_{0L}	-2.3	degree
α stall	20.02	degree
C_{Lmax} Landing	1.682	dimensionless

3. High Lift Devices

In the previous section it was found that the maximum obtainable CL was 1.682 which is quite a bit less than the previously selected landing CL of 2.4 and takeoff CL of 1.8. To supplement this deficit, high lift devices in the form of trailing edge and leading-edge devices such as flaps and slots can be employed.

3.1 Take-off and Landing conditions

Based on the required CL of 2.4 for landing and the found C_{Lmax} of 1.682, the high lift devices will need to provide a ΔC_{Lmax} of 0.718. This however would put the aircraft on the edge of a stall at such manoeuvres, so the ΔC_{Lmax} provided by the high lift devices will be designed around a

ΔC_{Lmax} of 0.818 to provide protection against gusts and manoeuvres. For takeoff it should be noted that the flaps will only be 60-80% effective due to the desire to not maximize drag as in the case of landing. This should be no problem though as even if the flaps are only 30% efficient, they should generate a ΔC_{Lmax} of 0.24 which when combined with the C_{Lmax} is greater than the required CL of 1.8.

3.2 High lift device approach selection

To obtain the required ΔC_{Lmax} , trailing edge devices will be sized to create the brunt of the ΔC_{Lmax} . Specifically, single Fowler flaps, as depicted in Figure 3.1, have been chosen as the trailing edge devices. This is due to their effective ability in creating a ΔC_{Lmax} while remaining operable at higher angles of attack than that of typical flaps. Specifically, the single slotted version was chosen over that of the double and triple slotted version due to the greatly reduced mechanical complexity. The single slotted version can provide the required delta and it may be harder to fit such complicated mechanisms on a smaller jet of this size. In addition to the trailing edge devices, leading edge devices in the form of slats will line much of the leading edge. As the trailing edge devices will be designed to be capable of providing the required ΔC_{Lmax} , the leading-edge devices will primarily be responsible for even further increasing the margin.

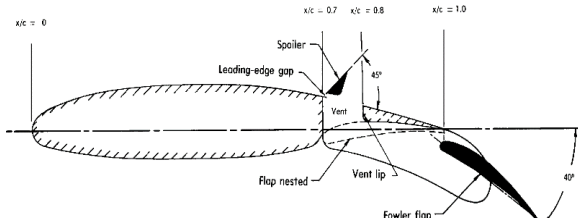


Figure 2.1: Example of Fowler Flap [3]

3.3 Device Sizing

The ΔC_{Lmax} provided by high lift devices can be found utilizing Equation 3.1 below.

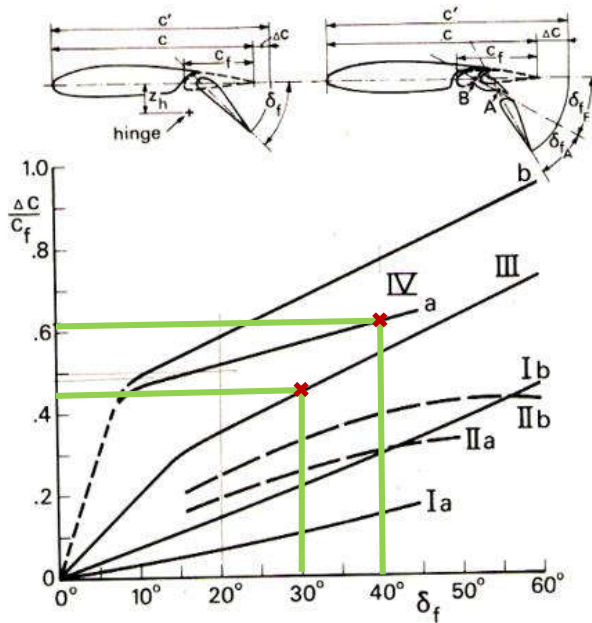
$$\Delta C_{Lmax} = 0.9 * \Delta C_{lmax} * \left(\frac{S_{fw}}{S} \right) * \cos(\Lambda_{hinge\ line}) \quad Eq.\ 3.1$$

Here the ΔC_{Lmax} is given as a requirement, the $\Lambda_{hinge\ line}$ is the sweep of the point of actuation for the device, the C_{lmax} is the Cl of the devices and S_{fw} is the area of the wing that has flaps on it, not to be confused with the flap area. The $\Lambda_{hinge\ line}$ can be found utilizing Eq. 2.11 where the x/c value can be estimated based on where the rear spar should be. The rear spar is estimated to be at $0.65c$, so the hinge point will be $0.05c$ back from that at $0.7c$ to provide room for actuation mechanisms. With that in mind, it can be found that the sweep at $0.7c$ is 11.38 degrees. ΔC_{lmax} values can be found using Figure 3.2 proposed by Raymer.

Here for Fowler flaps and slats it can be seen that a c'/c value is required. This value is the value of the chord of the wing with the flap extended over the chord of the clean wing. This value can be found using Figure 3.3 below. The delta f value is the deflection of the flap, which for this purpose will be set at a maximum deflection of 40 degrees. Note smaller values will be utilized for takeoff operations. From the figure, a $\frac{\Delta c}{c_f}$ value can be obtained. As depicted by the images at

Table 12.2 Approximate lift contributions of high-lift devices

High-lift device	$\Delta C_{l_{max}}$
Flaps	
Plain and split	0.9
Slotted	1.3
Fowler	1.3 c'/c
Double slotted	1.6 c'/c
Triple slotted	1.9 c'/c
Leading edge devices	
Fixed slot	0.2
Leading edge flap	0.3
Kruger flap	0.3
Slat	0.4 c'/c

Figure 3.2: $\Delta C_{l_{max}}$ Contribution of Various High Lift Devices [2]**Figure 3.3: Change in Chord Length per Flap Length Based on Deflection**

the top of the figure, this value is the change in wing chord over the clean wing chord. Curve IVa corresponds to that of a single Fowler flap. With that, a $\frac{\Delta C}{C_f}$ of 0.625 can be found. Multiplying this by the flap chord of 0.3c found from the hinge line, a ΔC value of 0.1875 is found. By adding 1, the c'/c value of 1.1875 can be found. Feeding this back through Figure 3.2, a $\Delta C_{l_{max}}$ of 1.544 is found. Finally, Eq. 3.1 can be rearranged into Equation 3.2 below to solve for S_{fw} .

$$S_{fw} = S * \frac{\Delta C_{l_{max}}}{0.9 * \Delta C_{l_{max}} * \cos(\Lambda_{hinge\ line})} \quad Eq. 3.2$$

The value of S_{fw} is found to be 27.75 m^2 or 60% of the wing surface area. With that the flap dimensions can be calculated. First, the wing chord of the root of the flap must be found. This can be done using Equation 3.3 where x is the location of the flap root and estimated to be 2.0265 m as to not intersect with the fuselage of the aircraft.

$$c_x = c_r - \left(\frac{c_r - c_t}{b/2} \right) x \quad Eq. 3.3$$

$c_{f\ root}$ is found to be 2.929 m long. This can now be utilized in Equation 3.4 presented below which takes advantage of geometrical relationships to find the single wing flap length.

$$l_{flap} = \frac{1}{\left(\frac{c_r - c_t}{b/2} \right)} (c_{f\ root} - \sqrt{c_{f\ root}^2 - \left(\frac{c_r - c_t}{b/2} \right) S_{fw}}) \quad Eq. 3.4$$

The flap length is found to be approximately 6.33 m per wing. The semi span of the wing can now be checked with the flap length to assure there is enough space to fit ailerons for roll control. With a semi span of 10.75 m, 6.33 m is utilized by flaps and 2.03 m is obstructed by the fuselage. That leaves a remaining 2.39 m of space for ailerons. The ailerons will be chosen to be 2 m wide placed towards the extremities of the wing but not right up against the wing tip. This should ensure enough controllability for the aircraft.

The above process can now be repeated for the leading-edge devices. The main difference this time is the S_{fw}/S is set at 0.8 as it is assumed that most of the leading edge will have slats on it and the generated ΔC_{Lmax} is to be calculated. The $\frac{\Delta c}{c_f}$ of the slats can be found utilizing curve III in Figure 3.3 and is found to be 0.45 at a set max deflection of 30 degrees. The c_f value is set at 0.15c to allow room for actuation mechanisms based on the estimated front spar position of 0.2c. Solving for c'/c in a similar fashion and plugging it into Figure 3.2 it is seen that a ΔC_{Lmax} of 0.427 is generated. Inserting all of this into Equation 3.1, an overall ΔC_{Lmax} of 0.292 is generated. This is relatively low, however, the main benefit of the leading-edge devices is their ability to extend the angle of attack at which the aircraft stalls.

3.4 CL-a Curve for Flapped Wing

Now that the contributions from the various high lift devices are better understood the Flapped CL-a curve may be constructed. One important difference for the flapped wing vs the clean wing is that the α_{0L} will be much lower due to the increase in effective angle of attack due to the extension and lowering of flaps. This $\Delta\alpha_{0L}$ can be found utilizing Equation 3.5 below where the delta 0 lift alpha of the airfoil is set to -10 for takeoff and -15 for landing.

$$\Delta\alpha_{0L} = (\Delta\alpha_{0L})_{airfoil} * \frac{S_{fw}}{S} * \cos(\Lambda_{hinge\ line}) \quad Eq. 3.5$$

With the S_{fw}/S value for the trailing edge devices and the found sweep angle the overall $\Delta\alpha_{0L}$ may be found to be -5.88 degrees for takeoff and -9.42 degrees for landing. Now the new slope, $C_{L\alpha}$ can be calculated. Utilizing Equation 3.6 the $C_{L\alpha\ flapped}$ can be found.

$$C_{L\alpha\ flapped} = C_{L\alpha\ clean} * \left(1 + \left(\frac{S_{fw}}{S} * c' \right) \right) \quad Eq. 3.6$$

4 slopes will be presented, 2 for both landing and takeoff configuration where 1 only has the contribution of trailing edge flaps and 1 has both leading edge and trailing edge devices

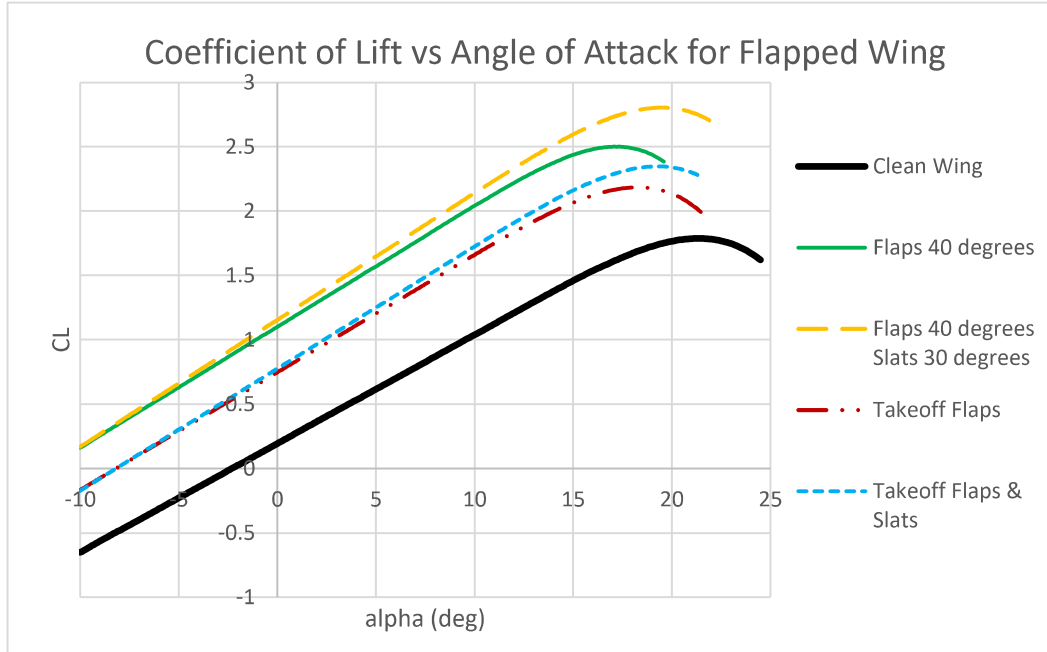


Figure 3.4: Flapped Wing CL-a curve

incorporated. All these values can be found in Table 3.1 below where all the flapped wing characteristics can be found. Lastly, before the curve may be displayed, the new stall angles must be calculated. Eq. 2.20 is once again utilized but this time with the flapped wing parameters that will once again be displayed in Table 3.1. With all these components, the full CL-a curve for the flapped wing in its various configuration can be seen in Figure 3.4. Note the ΔC_{Lmax} for takeoff configuration was estimated to be 60% that of the landing ΔC_{Lmax} .

Table 3.1: Flapped Wing Parameters

Parameter	Takeoff TE	Takeoff TE & LE	Landing TE	Landing TE & LE	Clean Wing	Unit
α_{0L}	-8.18	-8.18	-11.72	-11.72	-2.3	degrees
C_{La}	0.0913	0.0949	0.0940	0.0985	0.0845	CL/degree
C_{Lmax}	2.173	2.384	2.5	2.792	1.682	dimensionless
a_{stall}	17.34	19.20	17.28	20.39	20.02	degrees

4. Fuel Storage

From the above wing dimension, the volume available for fuel tanks can be. In this section the location and volumetric data of the fuel storage will be discussed, as well as additional adjustments and alternative locations and sizes of fuel tanks.

4.1 Wing Fuel Tank

Due to the high wing design and non-existent wing box within the fuselage, the primary fuel tank can be considered to be held entirely within the wing of the aircraft. The area where the fuel could be located was determined by the available area between the structural supports and limiting wing geometry. It is known that the span of the aircraft is 21.5m, or 10.75 meters per wing, and that the front and rear spars are located at 0.2c and 0.65c respectively. Typically fuel tanks take up a maximum of 85% of the wing due to limited space at the tips. With that in mind, the fuel tanks will be approximately 9.14m long in each half of the wing. The next step is to calculate the volume that the wing tanks can hold individually. To do so Equation 4.1 is presented.

$$V = \frac{L}{3} * (S_1 + S_2 + \sqrt{S_1 S_2}) \quad Eq. 4.1$$

S_1 and S_2 are the inner and outer trapezoidal faces of the roughly prismatic wing fuel tank, their respective values are found through Equations 4.2 a and b respectively. Figure 4.1 is presented below to better illustrate the meaning of these variables. From CAD, all the wing the necessary values were found and are displayed in Table 4.1 below.

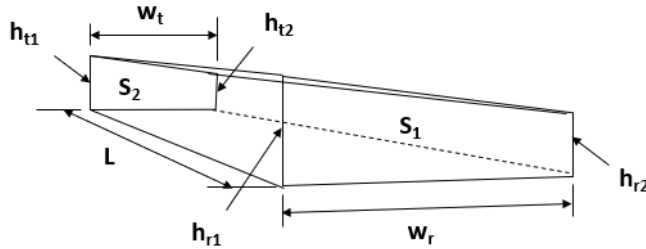


Figure 3.1: Wing Fuel Tank Estimated by Prism [1]

$$S_1 = \frac{1}{2} * (h_{r_1} + h_{r_2})w_r \quad Eq. 4.2 a$$

$$S_2 = \frac{1}{2} * (h_{t_1} + h_{t_2})w_t \quad Eq. 4.2 b$$

Table 4.1: Wing Fuel Tank Geometry

W_r	1.7 m
h_{r_1}	0.372 m
h_{r_2}	0.295 m
W_t	1.275 m
h_{t_1}	0.192 m
h_{t_2}	0.11 m
L	9.14 m
S_1	0.567 m
S_2	0.193 m

Plugging in the above values the volume can be calculated per wing. The absolute volume per wing comes out to be 3.32 m^3 . To find the actual total volume, that value must be doubled and multiplied by 91%. This is to account for 4% of the space being taken up by wing structures and



various systems and another 5% left empty to allow for the fuel to expand. The total wing fuel tank volume then comes out to be 6.04 m^3 .

4.2 Total Fuel Storage Capacity

With the above fuel tank volume, the weight of fuel that can be carried can be estimated. Jet A-1 fuel has a density of approximately 800 kg/m^3 . Multiplying this with the available volume of 6.04 m^3 a total mass of 4833.7 kg can be loaded. In terms of weight that is 47.42 KN of fuel. The previously calculated required amount of fuel was 32.79 KN. As the available room is well above the required volume there should be no issues accommodating the required fuel. With the extra room there are a few possibilities. First, extra fuel could be carried to extend range. Second, the excess space could be utilized to reinforce structures to better accommodate the high aspect ratio. Alternatively, the wing could be completely redesigned to have a thinner max thickness to optimize aerodynamic performance. Ultimately, the wing seems to be properly designed as a whole.



References

[1] W. De Backer, "Wing Sizing University of South Carolina, 2021.

AESP415_001_Fall2021_08-WingSizingV5

AESP415_001_Fall2021_08-WingSizingV5_Swf

[2] D. Raymer, *Aircraft design*. Reston: American Institute of Aeronautics and Astronautics, 2021.

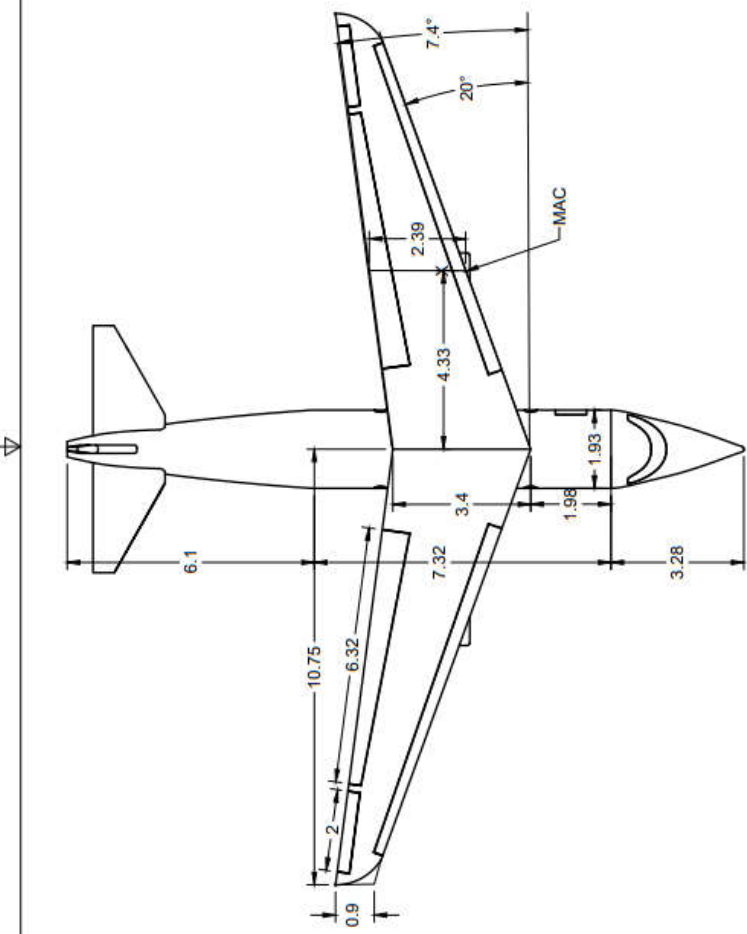
[3] J. Paulson, "Wind-tunnel investigation of a Fowler flap and spoiler for an advanced general aviation wing", www.semanticscholar.org, 1976. [Online]. Available: <https://www.semanticscholar.org/paper/Wind-tunnel-investigation-of-a-Fowler-flap-and-for-Paulson/9eb18dd307501b5a00055fd5789db87d5557b9b0> . [Accessed: 09- Nov- 2021].



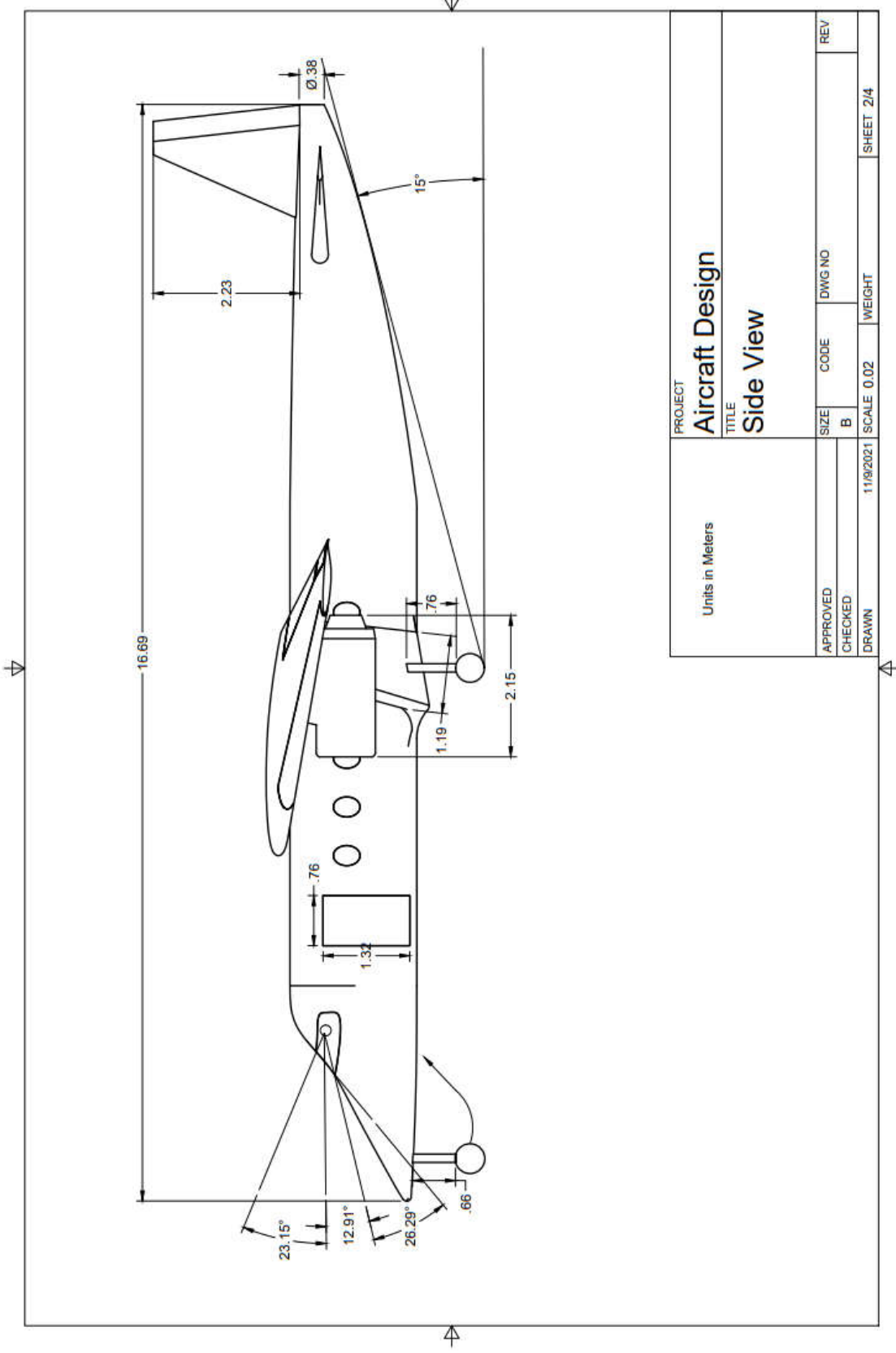
Appendix A: Updated Drawings

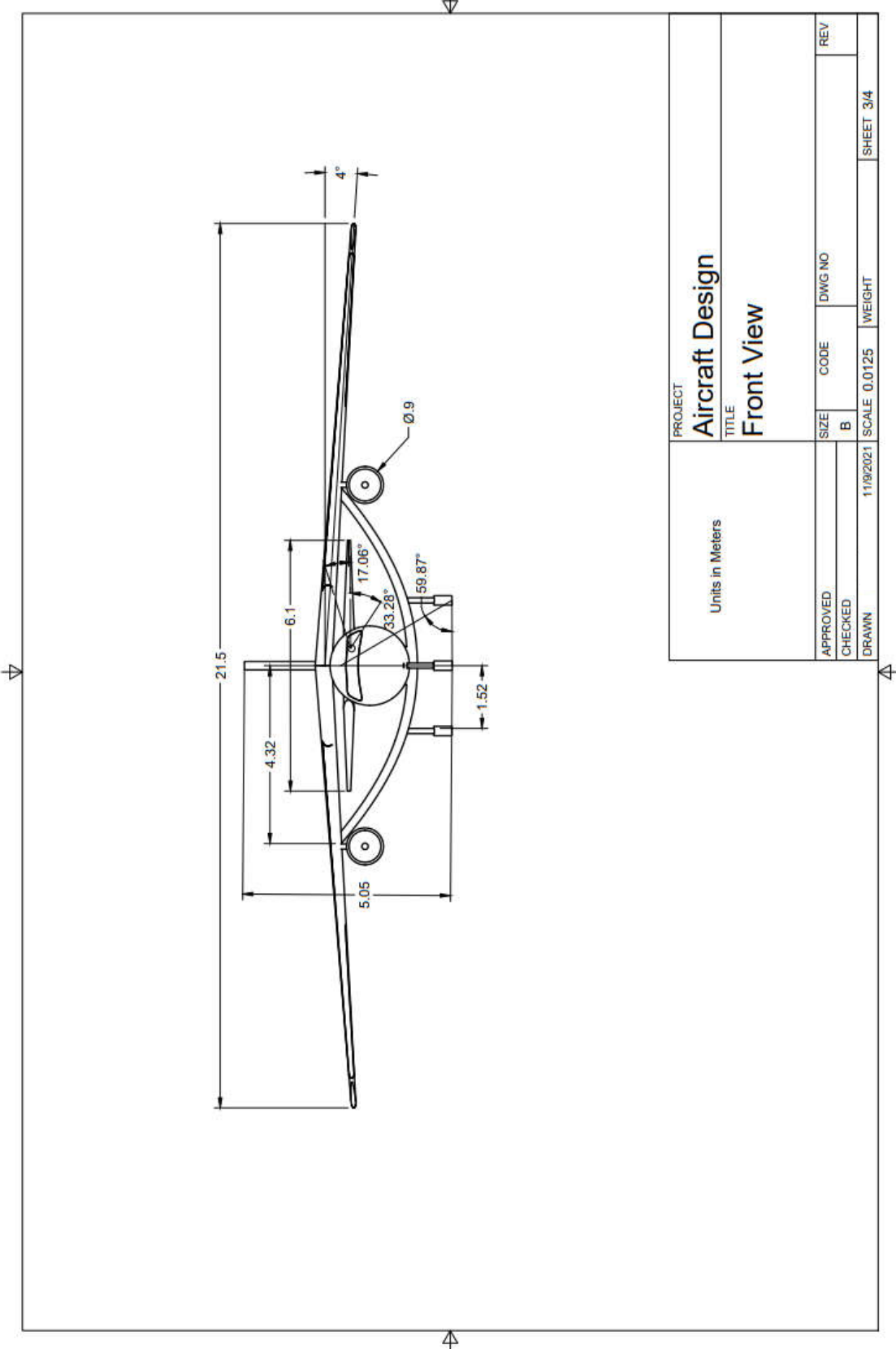
Below the technical Drawings for the aircraft are presented in the following order:

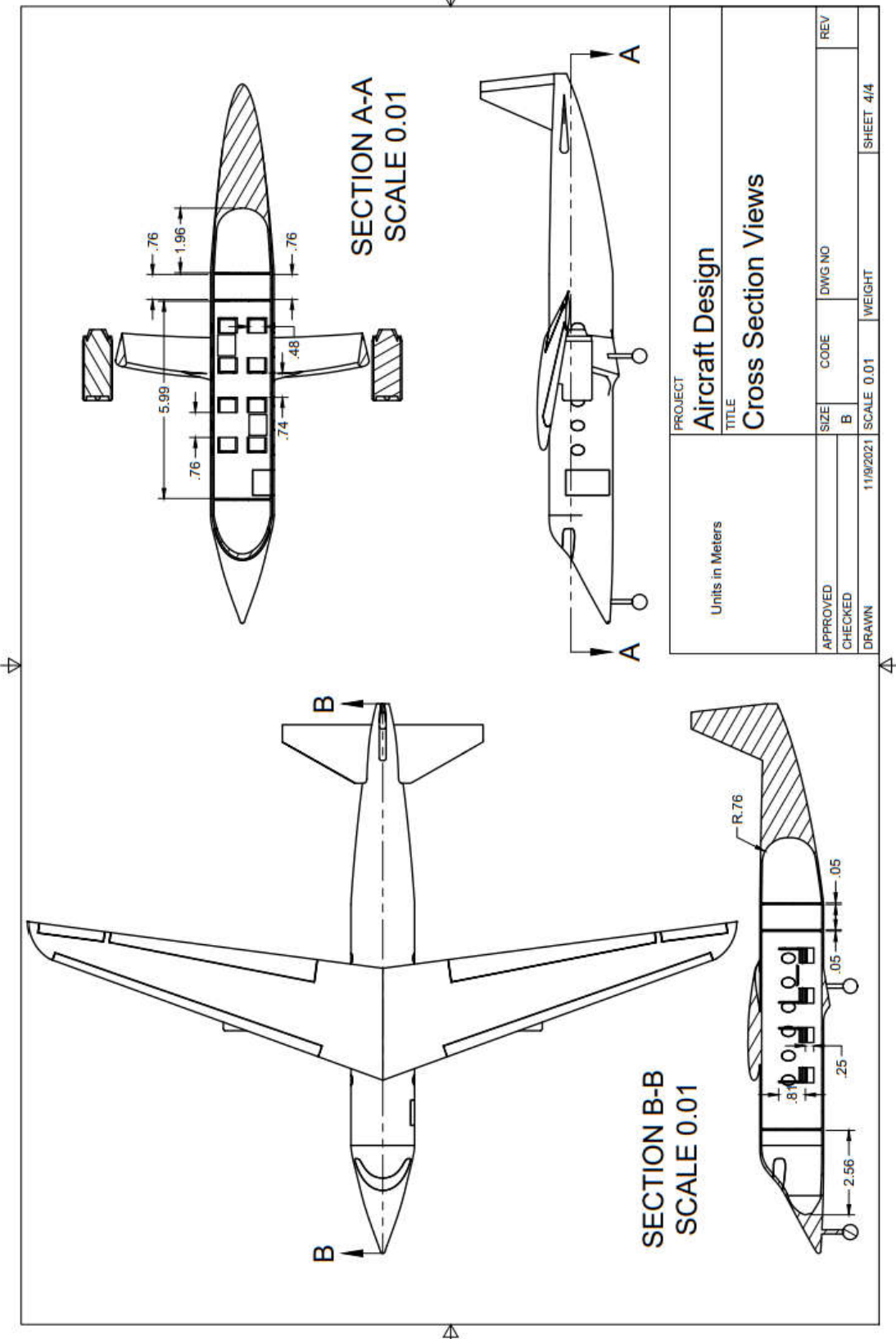
1. Top View
2. Side View
3. Front View
4. Cross Section Views
5. Fuselage Cross Section

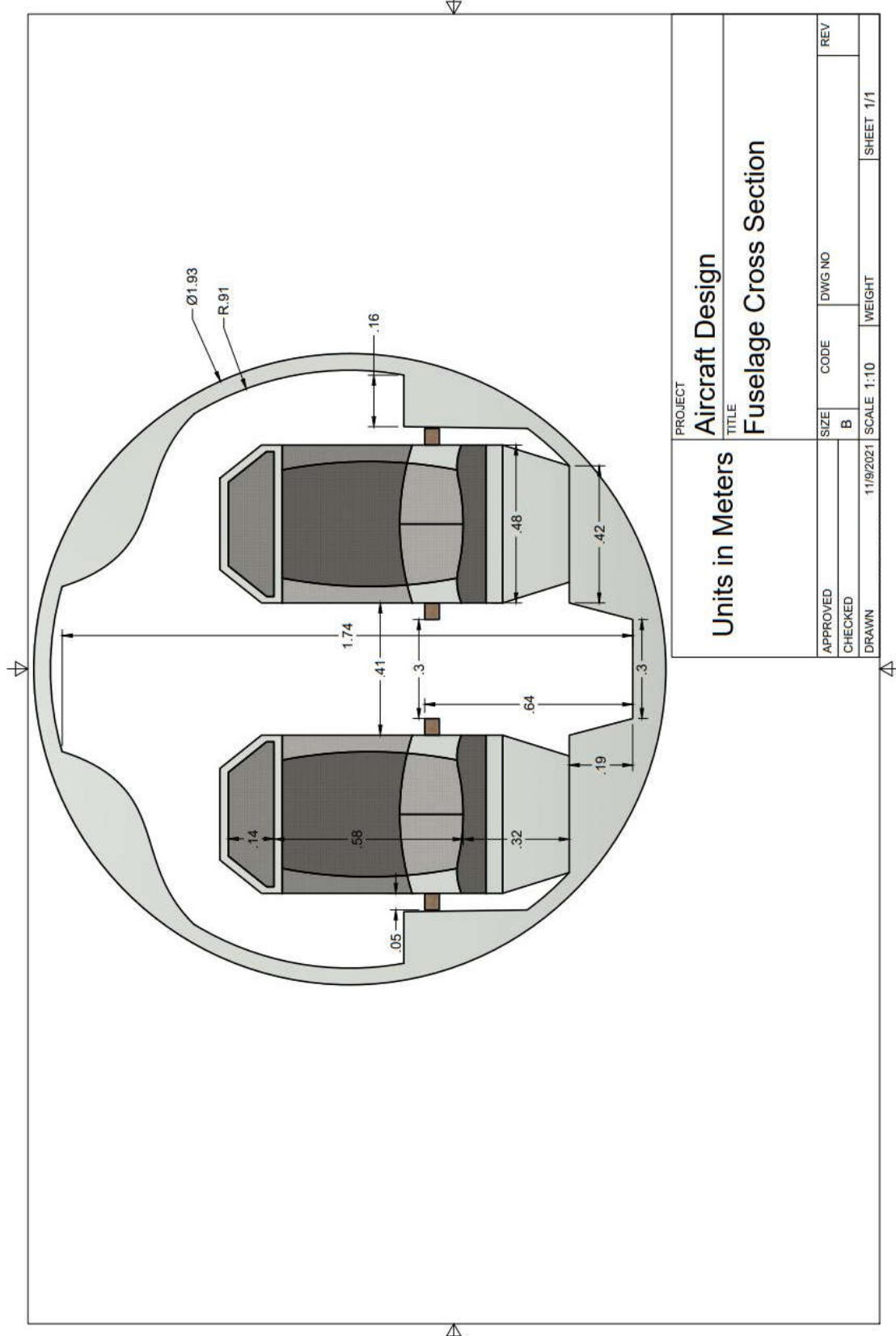


PROJECT		TITLE	
Aircraft Design		Top View	
Units in Meters			
APPROVED		SIZE	CODE
CHECKED		B	DWG NO
DRAWN		11/9/2021	REV
		SCALE 0.01	WEIGHT
			SHEET 1/4







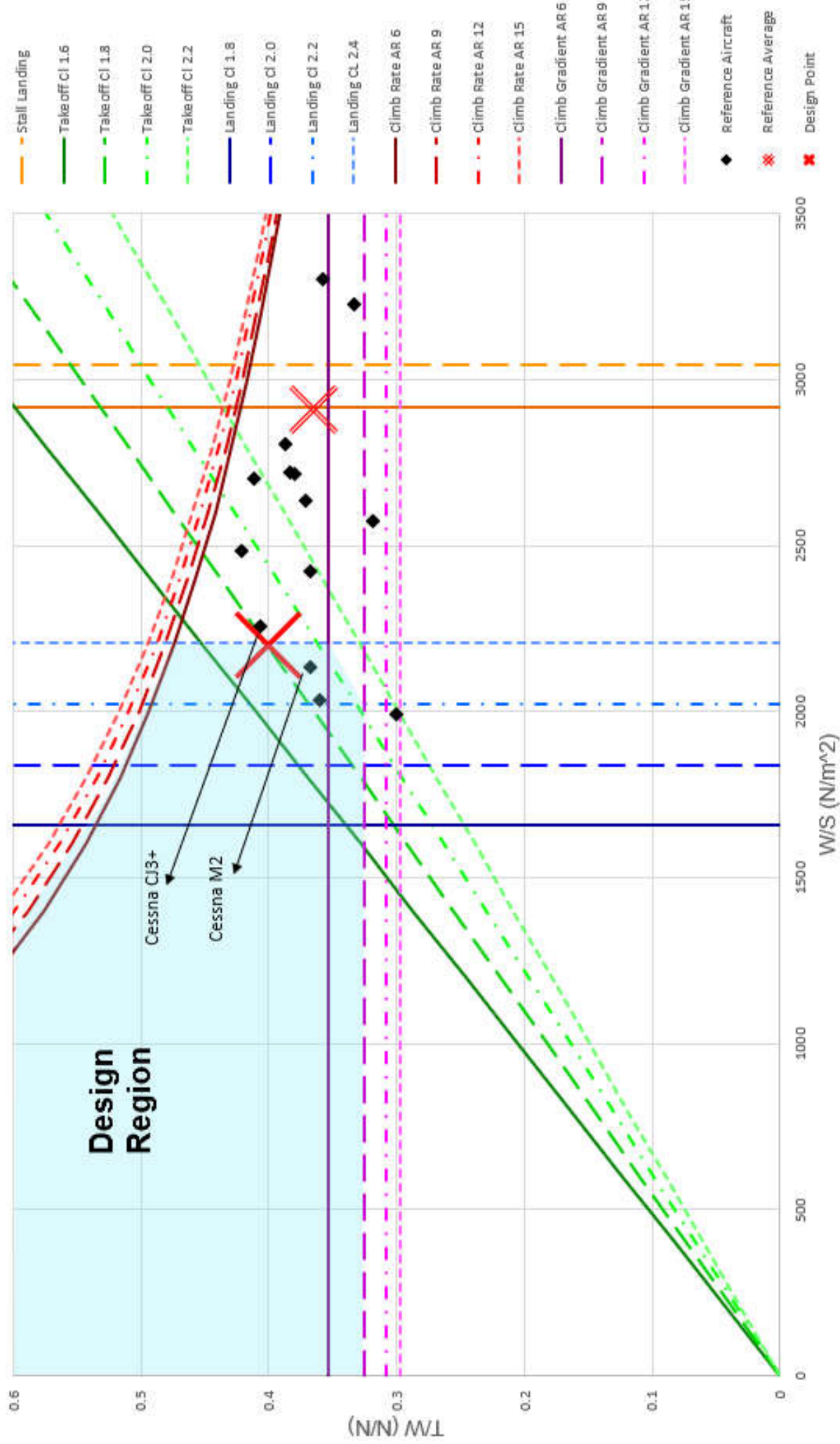




Appendix B: T/W – W/S graph

Below the Thrust Loading vs Wing Loading Graph is presented.

Thrust Loading vs Wing Loading



Appendix C: Table of Reference Aircraft

Aircraft Name	A/C Type	Payload [lb]	range [nm]	cruise speed [kn]	Height [ft]	Length [ft]	Wingspan [ft]	MTOW [lb]	Landing field length at max landing weight [ft]	Take off length Length (sea level) [ft]
105	Business Jet	1984.5	1728	415.77	16.25	54.5	40	TBD	2953	2624.8
CJ3+	Business Jet	1971.27	2040	416	15.16	51.15	53.35	13871.65	3179	2769.16
Cessna Citation CJ4	Business Jet	2220.44	2165	451	15.39	53.35	50.82	17113.00	3409	2939.77
Nextant 400XT	Business Jet	2469	2108	460	13.91	48.42	43.50	16300	3821	4045
Learjet 75	Business Jet	2902	2080	465	14.42	56.42	50.92	21500	4440	2296
Learjet 40	Business Jet	2305	1552	457	14.14	55.55	47.77	21000	4250	2660
Cessna Citation XLS+	Business Jet	2240.28	2100	441.14	17.06	52.50	56.33	21002.62	3560	3179.28
Phenom 300	Business Jet	2216	2077	430	16.41	52.12	53.12	17968	3138	3700
Eclipse 500/550	Business Jet	1800	1125.26	374.73	11.15	33.46	38.05	6000	2434.50	2788.85
Pilatus PC-24	Business Jet	2500.47	2000	440	17.38	55.12	55.77	18301.5	2929.93	2375.44
Pilatus PC-12	Business Jet	2235.87	1802.91	290	13.97	47.24	53.41	10451.7	2486.99	2168.74

Hawker 400	Business Jet	2000	1519	443	13.75	48.13	43.41	16300	3950	2960
Premier 1A	Business Jet	4000	1350	451	15.33	46	44.5	12500	3792	3170
HA-420	Business Jet	1400	1223	422	14.9	42.6	39.8	9964.39	3934	3047
Spectrum S-40 Freedom	Business Jet	2401.24	2200	440	11.81	53.8084	45.6059	9550	2998.83	2700.26
Stratos 714/716X	Business Jet	2160.9	1777	415	11.41	35.79571	40.48754	8423.1	2089.99	1509.26
Syberjet SJ30	Business Jet	1500	2129	436	14.20	46.78706	42.3249	13951.03	3937.2	2552.61
Gulfstream G150	Business Jet	2400	3130	459	19.08	56.75	55.583	26100	5012	2431
Predator 500	Business Jet	1680.21	3250	466	21.08	64.583	70.5	37567	4222.64	2091
Phenom 100EV	Business Jet	1000	1178	406	14.27	42.06242	40.3563	10852	3190	2430
Learjet 60	Business Jet	2200	2408.74	453	14.5	58.583	43.66	23500	5920	3120
Fairchild Dornier 328JET	Business Jet	2952	1800	400	23.12	69.65563				
Citation Latitude	Business Jet	2544	2699.78	446	20.93	62.24057	72.34605	34530.3	4485.12	4284.98
Citation M2	Business Jet	1510.42	1550.21	403.88	13.91	42.58738	47.2464	10700.86	3208.81	2590
	AVERAGE:				15.53	51.08	50.33	17750.14		

Appendix D: Current Aircraft parameters Table

Symbol	Parameters	Value	Unit
Flight Parameters			
h_{cruise}	Cruise altitude	12192	m
V_{cruise}	Cruise speed	770	km/h
CL_{cruise}	Cruise lift coefficient	1.8	
CL_{max}	Max lift coefficient	2.6	
s_{TO}	Take-off distance	900	m
S_L	Landing distance	800	m
R	Range	3200	km
Weight Parameters			
W_{MTOW}	Maximum Take-off Weight	101.7	kN
W/S	Wing Loading	2200	N/m ²
T/W	Thrust to weight ratio	0.4	
W_F	Fuel Weight	32.79	kN
W_{BO}	Basic operating weight	62.9	kN
Power Plant Parameters			
T	Take-off Thrust	20.4	kN
D	Fan Diameter	906	mm
L	Length	1933	mm
W dry	Dry Weight	392	kg
	SFC Cruise	0.07239	kg/N*h